# Reports

## $^{40}Ar$-$^{39}Ar$ Dating of the Manson Impact Structure: A Cretaceous-Tertiary Boundary Crater Candidate

M. J. Kunk, G. A. Izett, R. A. Haugerud, J. F. Sutter

**The mineralogy of shocked mineral and lithic grains in the Cretaceous-Tertiary (K-T) boundary claystone worldwide is most consistent with a bolide impact on a continent. Both the concentrations and sizes of these shocked grains are greatest in the western interior of North America. These data suggest that the Manson impact structure in north-central Iowa is a viable candidate for the K-T boundary impact event. Argon-40–argon-39 age spectrum dating of shocked microcline from the crystalline central uplift of the Manson impact structure indicates that there was severe argon-40 loss at 65.7 ± 1.0 million years ago, an age that is indistinguishable from that of the K-T boundary, within the limits of analytical precision.**

On the basis of an unusually high concentration of iridium in a claystone layer that occurs at the K-T boundary in outcrops of marine rocks in Italy, Denmark, and New Zealand, Alvarez *et al.* hypothesized that the extinctions that occurred at the K-T boundary were the result of an asteroid impact (*1*). The iridium anomaly that they described has now been detected at many other K-T boundary locations throughout the world (*2*). The hypothesis that an impact was the cause of extinctions at the K-T boundary is still being debated, and a competing hypothesis suggests that the extinctions and many features of the K-T boundary layer can best be explained to be a result of large-scale volcanism (*3*). One of the uncertainties regarding the impact hypothesis is the location of the impact crater. Using the concentrations detected, Alvarez *et al.* suggested that the impacting bolide was 10 ± 4 km in diameter. The impact of a bolide of this size would have resulted in a crater ≈100 km in diameter.

Geochemical data on material from the K-T boundary interval in marine sections suggested that the impact was probably in oceanic crust (*4*), in which case it may have been subducted. This interpretation was challenged following the recognition of shock-metamorphosed mineral and lithic grains in the K-T boundary claystone (*5, 6*). Shocked grains include quartz, quartzite and metaquartzite, oligoclase, microcline, and granite-like oligoclase-microcline-quartz lithic grains (*5, 6*). The mineralogy and cathodoluminescence (*7*) of the boundary layer clastic grains and their relative proportions suggest that an impact occurred in an area dominated by continental sedimentary and metasedimentary rocks. The presence of trace amounts of shock-metamorphosed oligoclase, microcline, and granite-like lithics suggests that the target rocks also included some granitic rocks or continental crystalline basement. The shock features preserved in these grains include multiple sets of intersecting planar lamellae, shock mosaicism, lowered refractive indices and birefringence, and shock-induced fluid inclusions (*6*). Although it has been argued that shock features could be produced by volcanism (*3*), multiple intersecting sets of planer lamellae are characteristic of shocked grains found in impact environments and have never been described in volcanic rocks (*8*).

The general location of a continental impact site can be inferred from data on the maximum grain size and relative abundance of shocked grains in the K-T boundary claystone (*6*). Shocked grains in the claystone are more abundant in the western interior of North America than elsewhere and the maximum size of the shocked grains is also significantly greater in western North America (*6*).

On the basis of these data, a likely candidate is the Manson impact structure (MIS) (*9*). The MIS is located in northwestern Iowa, about 30 km west of Fort Dodge near the town of Manson, and has a diameter of about 35 km; it is the largest known impact structure in the United States. It is covered with 30 to 90 m of Pleistocene glacial till and has no obvious topographic expression. Much of what is known of the MIS has been learned from the study of shallow well cuttings.

The basement rocks in the MIS area are composed of Proterozoic garnetiferous-oligoclase-biotite-quartz gneiss, which was intruded by granite at about 1450 million years ago (Ma). Both are crosscut by diabase dikes, probably of Keweenawan age (~1000 Ma). The crystalline basement is covered by a thick sequence of Precambrian to Mesozoic sedimentary rocks including sandstone, conglomerate, shale, fluvial sedimentary rocks, and marine carbonate and clastic rocks (*9*). The thick Precambrian clastic rocks thin abruptly to the northwest, and total sedimentary rock thickness ranges from 3700 m on the northwest of the MIS to 7500 m on the southeast (*9*). The composition of the target rocks at Manson is consistent with that of shocked grains found in the K-T boundary claystone.

The center of the MIS has been uplifted, and crystalline basement is at the level of the glacial subcrop. The sedimentary rocks surrounding the central uplift have been completely disrupted and are characterized by exotic (metamorphic and igneous) lithologies and severe deformation. This region is surrounded by a region where the strata have retained their original depositional sequence but have been displaced vertically. Down-dropped blocks in this zone locally preserve Cretaceous marine shale. The total diameter of these three zones is about 35 km. The rocks in the surrounding 10 to 16 km have been slightly uplifted (*9*).

The MIS was originally interpreted to be a cryptovolcanic (cryptoexplosive) structure (*10*). Interpretation as an impact structure is based on the discovery of multiple intersecting sets of shock lamellae in quartz from the rocks of the crystalline uplift (*11*) and its overall morphology. The MIS has been thought to be Cretaceous in age because Mesozoic fish scales and Cretaceous *Inoceramus* fossils have been found in the rocks of the disrupted zone (*12*).

Paleomagnetic data from the MIS central uplift core, however, suggest that it cannot be associated with the K-T boundary. The K-T boundary is known to have occurred during chron 29R, a time when the earth was in a period of reversed magnetic polarity (*13*). Hypervelocity shock accompanying an impact could reset the remanent magnetic field of a rock to that of the ambient field at the time of impact (*14*). Thus, in this case, if the MIS was formed at the time of the K-T boundary, the shocked rocks could have a reversed magnetic polarity. Paleomagnetic polarities from four lithologies at three different levels in the core have been determined (*15*). The two upper samples contain a normal component of magnetization. The

M. J. Kunk and J. F. Sutter, U.S. Geological Survey, Reston, VA 22092.
G. A. Izett, U.S. Geological Survey, Denver, CO 80225.
R. A. Haugerud, U.S. Geological Survey, Menlo Park, CA 94025.

two lithologies lower in the core record a more complex natural magnetic remanence that was interpreted to represent a normal polarity at the time of impact with a possible Precambrian remanence that survived the impact event. There are, however, several reasons to question this interpretation of the data (*16*). The intense deformation that occurs during the formation of a central uplift includes wholesale block rotation. Some or all of the reported magnetic polarities could simply represent blocks that have been inverted. An alternative interpretation of the data from the deepest samples suggests that a reverse overprint may be present. Finally, the observed normal polarity might represent viscous magnetization acquired after the impact event. A thorough study of the paleomagnetic polarity of the shocked rocks in the MIS is needed before the paleomagnetic data can be accepted as strong evidence against a K-T boundary age for the MIS. Until additional data are available, a connection between the K-T boundary impact layer and the MIS cannot be ruled out.

One could argue that the MIS could not have produced the worldwide K-T boundary deposits simply on the basis of its size. Alvarez *et al.* (*1*) estimated that the K-T boundary crater would have been about 100 km in diameter, but the MIS is only about 35 km in diameter. However, because of the number and range of variables possible for any one impact (*6*), the diameter of the single crater of the Alvarez *et al.* hypothesis cannot be estimated precisely with available data. Furthermore, if multiple impacts occurred at the K-T boundary, then the diameter of any single crater is clearly undefined.

Earlier dating of materials from the central uplift core has hinted at the age of the MIS. Severely microfractured apatite grains from the core of the MIS yielded a fission track age of 61 ± 18 Ma (*17*). When compared with fission track ages of apatite grains from basement material taken from a drill core in northwestern Iowa, which range from 641 ± 90 to 934 ± 86 Ma (*18*), the dramatically younger ages suggest that the Manson apatite age was reset at the time of impact. Similarly, $^{40}Ar$-$^{39}Ar$ age spectrum dating results from shocked potassium feldspar from the 70.4-m level in the core (*17*) suggest that the maximum age for the impact is ~70 Ma. These ages are similar to the age of the K-T boundary.

Because of the uncertainty in the age of the crater, we have dated two potassium feldspar samples from granitic materials at the 61.0- and 131.1-m levels (*19*) in the MIS central uplift core with $^{40}Ar$-$^{39}Ar$ age spectrum dating techniques (*20–23*). At these levels, the core is a coherent shocked granite composed of quartz, potassium feldspar, plagioclase, and chloritized biotite. X-ray diffraction analysis of potassium feldspar grains separated from our samples (*24*) show that they are composed of maximum microcline having about 3 to 4% (2A200) and 10 to 15% albite (2A430) (*25*). The mechanism by which the argon systems of potassium feldspars are reset during shock metamorphism has not been directly determined. Experimental data show that plagioclase, when subjected to high levels of shock and then quenched, does not lose radiogenic $^{40}Ar$, indicating that shock-induced heating is responsible for the $^{40}Ar$ loss (*26*). If these results also apply for microcline, the mechanism of $^{40}Ar$ loss is most likely shock-induced heating and subsequent cooling through its argon retention temperature. Maximum microcline is especially useful in this type of study because it has a relatively low temperature for argon closure and degasses by simple volume diffusion (*27*).

The overall shape of the age spectra for the two samples, although similar, differs in detail (Fig. 1 and Table 1). We first analyzed 2A200, and the heating schedule used for degassing the sample did not give us enough

**Table 1.** $^{40}Ar$-$^{39}Ar$ analytical data for MIS microcline samples 2A200 and 2A430 (*35*); $^{40}Ar_R/^{39}Ar_K$ ratios represent radiogenic $^{40}Ar$ and potassium-derived $^{39}Ar$ after corrections for mass discriminations, the presence of atmospheric argon, and the production of interfering argon isotopes during neutron irradiation (*22, 23*). $^{39}Ar_K$ concentrations were calculated by use of the measured sensitivity of the mass spectrometer and thus are reproducible to about 5% based on repeated measurements of MMHb-1 spaced over a period of 8 months. Errors of individual temperature steps (1 SD) are calculated from standard statistical methods on five sets of argon peak values measured over an interval of about 10 min by the method described in (*22*). No error is calculated for the total gas age. The uncertainty of the preferred age (2 SD) includes the 1 SD uncertainty in the irradiation parameter, *J*, as described in (*22*). This uncertainty has been quadratically combined with the published uncertainty in the age of the monitor mineral MMHb-1 (*34*). For both samples, $J$ = 0.005710 ± 0.5 (1 SD); sample weights were 0.1440 g for 2A200 and 0.1448 for 2A430; *T*, temperature.

| *T* (°C) | $^{40}Ar_R/^{39}Ar_K$ | Apparent K/Ca | Percent $^{39}Ar$ | Radiogenic yield (%) | $^{39}Ar_K$ ($10^{-13}$ mole) | Apparent age (Ma) |
|---|---|---|---|---|---|---|
| | | | *2A200 Microcline* | | | |
| 450 | 7.331 | 74 | 2.3 | 97.5 | 6.61 | 73.98 ± 0.69 |
| 500 | 7.319 | 100 | 6.7 | 98.9 | 19.6 | 73.86 ± 0.22 |
| 550 | 6.989 | 121 | 17.2 | 99.3 | 50.4 | 70.59 ± 0.18 |
| 600 | 6.614 | 128 | 29.7 | 99.5 | 87.2 | 66.87 ± 0.07 |
| 625 | 6.769 | 95 | 8.9 | 99.4 | 26.2 | 68.42 ± 0.10 |
| 650 | 6.959 | 104 | 4.1 | 97.2 | 12.0 | 70.30 ± 0.25 |
| 700 | 7.190 | 82 | 3.2 | 89.8 | 9.36 | 72.59 ± 0.58 |
| 750 | 7.365 | 102 | 2.0 | 97.5 | 5.89 | 74.32 ± 0.74 |
| 800 | 7.576 | 49 | 2.1 | 97.2 | 6.31 | 76.40 ± 0.62 |
| 850 | 8.280 | 41 | 1.7 | 98.3 | 5.06 | 83.34 ± 0.32 |
| 900 | 9.015 | 32 | 1.2 | 97.0 | 3.57 | 90.55 ± 1.10 |
| 950 | 10.190 | 75 | 0.9 | 96.2 | 2.79 | 102.02 ± 1.83 |
| 1000 | 12.271 | 37 | 0.8 | 97.0 | 2.39 | 122.17 ± 1.26 |
| 1050 | 14.218 | 75 | 1.1 | 96.7 | 3.15 | 140.82 ± 1.35 |
| 1150 | 12.892 | 37 | 4.0 | 98.7 | 11.7 | 128.14 ± 0.69 |
| 1250 | 14.926 | 20 | 14.1 | 98.0 | 41.3 | 147.54 ± 0.16 |
| | | | | | Total gas age | 85.1 |
| | | | Minimum age (29.7% of gas in 600°C step) | | | 66.87 |
| | | | *2A430 Microcline* | | | |
| 450 | 7.080 | 23 | 3.2 | 97.1 | 6.38 | 71.50 ± 0.85 |
| 500 | 6.859 | 34 | 8.4 | 98.8 | 16.7 | 69.30 ± 0.50 |
| 525 | 6.658 | 38 | 7.1 | 98.8 | 14.2 | 67.31 ± 0.48 |
| 550 | 6.516 | 38 | 11.4 | 99.2 | 22.9 | 65.90 ± 0.33 |
| 565 | 6.425 | 34 | 11.5 | 99.2 | 23.1 | 65.00 ± 0.38 |
| 575 | 6.528 | 23 | 5.4 | 99.3 | 10.8 | 66.02 ± 0.46 |
| 590 | 6.554 | 18 | 4.5 | 98.1 | 9.01 | 66.28 ± 0.93 |
| 600 | 6.755 | 13 | 2.3 | 98.3 | 4.54 | 68.27 ± 1.08 |
| 650 | 6.970 | 14 | 3.1 | 99.0 | 6.28 | 70.41 ± 0.47 |
| 700 | 7.125 | 11 | 3.0 | 97.8 | 5.97 | 71.94 ± 1.55 |
| 750 | 7.659 | 13 | 6.3 | 91.3 | 12.6 | 77.22 ± 0.16 |
| 850 | 9.012 | 22 | 11.6 | 98.2 | 23.2 | 90.52 ± 0.42 |
| 950 | 14.131 | 9 | 2.4 | 98.3 | 4.88 | 139.99 ± 1.45 |
| 1050 | 25.706 | 6 | 2.4 | 97.7 | 4.76 | 247.07 ± 0.32 |
| 1150 | 28.036 | 4 | 7.0 | 98.9 | 14.0 | 267.88 ± 0.24 |
| 1200 | 34.695 | 11 | 8.9 | 99.3 | 17.8 | 326.07 ± 0.54 |
| 1250 | 45.020 | 5 | 1.5 | 97.4 | 2.92 | 412.71 ± 1.71 |
| | | | | | Total gas age | 121.35 |
| | | | Preferred age (32.9% of gas in 550° to 590°C steps) | | | 65.7 ± 1.0 |

resolution. The analysis of 2A430 was performed with the results of 2A200 in hand, and the heating schedule used was much more appropriate. The results of both analyses display the same general features (*28*): the apparent ages in the very low temperature portion (450° to 525°C) of the spectra decrease with increasing temperature; the apparent age is constant (in 2A430) within the limits of analytical precision in the low-temperature portion (550° to 590°C) of the spectra; the apparent age rapidly increases with increasing extraction temperature in the higher temperature steps (600° to 1250°C). The trend of decreasing apparent age with increasing degassing temperature for the first five steps of 2A430 and first four steps of 2A200 suggests that the slightly older apparent ages calculated for these steps reflect the pressure of $^{40}$Ar-enriched intergranular argon at the time of degassing (*22*).

These age spectra (especially 2A430) are similar to Turner's (*29*) theoretical diffusion curves for argon loss from a log-normal distribution of spheres ($\sigma = 0.6$) and a 98% argon loss. In Turner's diffusional-loss model, the apparent age of low-temperature portions of gas released during analysis corresponds to the age of degassing (in our samples, the time of impact). The apparent age of the gas released in the last step approaches, although may not equal, the age of initial closure to argon diffusion (the age of our samples before impact). The shape of the age spectrum between initial and final gas release reflects the extent of degassing and the grain-size distribution in the sample. For samples that have a large amount of argon loss, the portion of the age spectrum that can represent the age of the resetting event, within the limits of analytical precision, can equal or exceed 50%.

Our samples have a small amount of extraneous argon in the low-temperature portion of their age spectra, thus complicating our ability to measure precisely the age of the degassing event. Additionally, the best estimates of the initial age of our sample range from 934 to 641 Ma (based on a $^{40}$Ar closure temperature for maximum microcline similar to the fission track annealing temperature of apatite) and have an absolute minimum of 413 Ma for 2A430 (apparent age of last heating step). These factors, together with the presence of impurities and uncertainties concerning the effective grain size distribution (*28*) in these samples, make a critical comparison with a theoretical diffusional loss model somewhat difficult. We have nonetheless made such a comparison (*30*) (Fig. 2); the diffusional loss model cannot be used to predict the age of the degassing event because of the factors mentioned above, and its value is instead qualitative. The experimental data departs from the theoretical diffusion curve in two temperature ranges, 450° to 525°C and 950° to 1050°C. The 450° to 525°C steps, as was mentioned above, contain extraneous argon, resulting in an increase in apparent age that is not supported by the potassium content of the sample. The apparent K/Ca ratio (Table 1) of the gas released in the 950° to 1050°C range suggests that the high-temperature departure from the theoretical diffusion curve most likely results from the presence of albite in the sample. This interpretation is consistent with theoretical diffusion profiles of two component mixtures with differing activation energies for argon diffusion (*31*). This departure from the Turner diffusion model is small when compared with the overall fit. In both theoretical diffusion models, however, the gas released in the low-temperature portion of the age spectrum (which in 2A430 does have apparent K/Ca ratios consistent with those of microcline) is expected to represent the age of the resetting event. A comparison between our data and the diffusion models support our interpretation that this age spectrum was caused by a single episodic degassing of ~95% of the radiogenic argon previously contained in the sample.

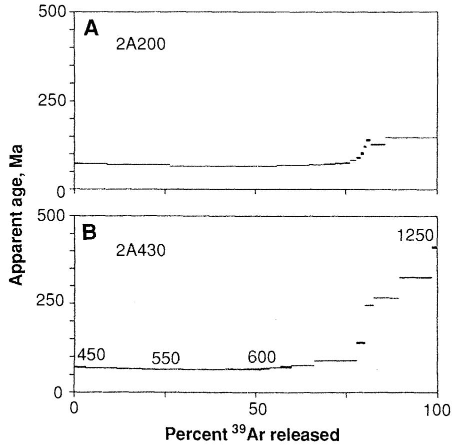


**Fig. 1.** $^{40}$Ar/$^{39}$Ar age spectrum diagrams of microcline samples (**A**) 2A200 and (**B**) 2A430 from core in central uplift of the MIS.

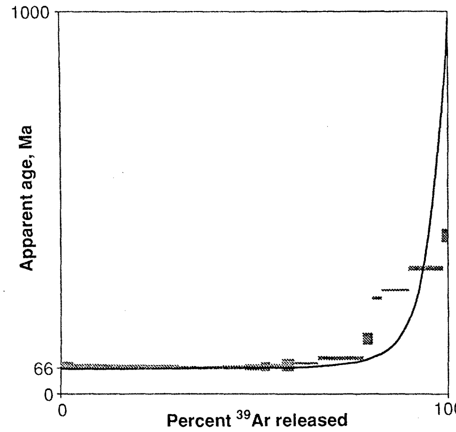


**Fig. 2.** Composite diagram of $^{40}$Ar-$^{39}$Ar age spectrum of 2A430 and calculated theoretical diffusive loss curve, calculated for an initial age of 934 Ma and a log-normal distribution of spheres that have $\sigma = 1.2$. Models for lower possible initial ages suggest that $\sigma$ is larger in these cases. For further details see (*30*).

The best estimate for the time of the Manson impact is the integrated age of the 550° to 590°C steps of 2A430, which agree within the limits of analytical precision, at 65.7 ± 1.0 Ma (see Table 1) and represent 33% of the total $^{39}Ar_K$ derived from the sample. Interpreting this age spectrum as a severe diffusive loss with a small amount of superimposed extraneous $^{40}$Ar implies that 65.7 ± 1.0 Ma is a maximum age. However, it is unlikely that the age of impact is significantly younger because four contiguous steps (550° to 590°C) agree in age with one another within the limits of analytical precision, contain one third of the $^{39}$Ar released, and occur in that portion of the age spectrum pattern in which theoretical diffusion models suggest that the age should essentially be equal to that of the degassing event. The minimum in the age spectrum of 2A200 (66.9 Ma) is supportive also of this interpretation. This sample may have incurred a higher degree of degassing than 2A430 as indicated by its younger high temperature and total gas $^{40}$Ar-$^{39}$Ar ages. Even so, the minimum step age of this sample is likely to be contaminated by a small amount of extraneous $^{40}$Ar.

Our 65.7 ± 1.0 Ma age for the MIS is indistinguishable from recent estimates for the age of the K-T boundary that range from 65 to 66.0 Ma (*32*), as well as our own estimate of the K-T boundary age of 66.0 Ma (*33*). The type and distribution of shocked mineral grains in the K-T boundary layer indicate that an impact in the western interior of North America is of high probability, and the lithologic assembly at the MIS is consistent with that of the shocked minerals in the K-T boundary layer. On this basis we conclude that the MIS is a viable candidate for a K-T boundary impact site and that intensive study of the MIS and other impact structures that could be of K-T boundary age is warranted.

REFERENCES AND NOTES

1. L. W. Alvarez, W. Alvarez, F. Asaro, H. V. Michel, *Science* **208**, 1095 (1980).
2. R. Ganapathy, *ibid.* **209**, 921 (1980); J. Smit and J. Hertogen, *Nature* **285**, 198 (1980); F. T. Kyte, Z. Zhou, J. T. Wasson, *ibid.* **288**, 651 (1980); S. Gartner and M. J. Jiang, *Earth Planet. Sci. Lett.* **54**, 393 (1981); C. J. Orth *et al.*, *Science* **214**, 1341 (1981); J. M. Luck and K. K. Turekian, *ibid.* **222**, 613 (1984); W. Alvarez, and A. Montanari, *Geol. Soc. Am. Abstr. Progr.* **17**, 512 (1985); F. T. Kyte, J. Smit, J. T. Wasson, *Earth Planet. Sci. Lett.* **73**, 183

(1985); F. E. Lichte *et al.*, *Nature* **322**, 816 (1986).
3. N. L. Carter, C. B. Officer, C. A. Chesver, W. I. Rose, *Geology* **14**, 380 (1986).
4. D. J. Depaolo *et al.*, *Earth Planet, Sci. Lett.* **64**, 356 (1983).
5. G. A. Izett and C. I. Pillmore, *Eos* **66**, 1148 (1985); G. A. Izett, *Geol. Soc. Am. Bull.* **99**, 78 (1987).
6. G. A. Izett, *U.S. Geol. Surv., Open-File Rep. 87-606* (1987).
7. M. R. Owen and M. H. Anders, *Nature* **334**, 145 (1988).
8. G. A. Izett and B. F. Bohor, *Geology* **15**, 90 (1987); J. S. Alexopoulos, R. A. F. Grieve, P. B. Robertson, *ibid.* **16**, 796 (1988).
9. J. Hartung and R. Anderson, *Lunar Planet. Inst. Tech. Rep. 88-08* (1988).
10. R. A. Hoppen and J. E. Dryden, *Geology* **66**, 694 (1958).
11. N. M. Short, *Geol. Educat.* **16** (no. 4), 149 (1966).
12. W. E. Hale, *Iowa Geol. Surv. Water Supply Bull. 4* (1955).
13. W. Alvarez *et al.*, *Geol. Soc. Am. Bull.* **88**, 383 (1977); W. Lowrie and W. Alvarez, *ibid.*, p. 374; E. M. Shoemaker, C. L. Pillmore, E. W. Peacock, *Geol. Soc. Am. Spec. Pap.* **209**, 131 (1987).
14. S. M. Cisowski and M. Fuller, *J. Geophys. Res.* **83**, 3441 (1978).
15. S. M. Cisowski, *Lunar and Planet. Sci.* **XIX**, 188 (1988).
16. E. M. Shoemaker, written communication.
17. J. B. Hartung *et al.*, *Lunar and Planet. Sci.* **XVII**, 313 (1986).
18. K. D. Crowley, C. W. Naeser, C. A. Babel, *Earth Planet. Sci. Lett.* **79**, 329 (1986).
19. In 1953, a joint U.S. Geological Survey–Iowa Geological Survey drilling project recovered core from near the center of the structure. The upper 28.3 m of the hole was in glacial till and was not recovered. Core ran the remainder, to a depth of 146.0 m and is mostly crystalline metamorphic and igneous rocks from the central uplift that have been intensely fractured and brecciated but are otherwise representative of the local basement rocks.
20. G. B. Dalrymple and M. A. Lanphere, *Earth Planet. Sci. Lett.* **12**, 300 (1971).
21. G. B. Dalrymple *et al.*, *U.S. Geol. Surv. Prof. Pap. 1176* (1981).
22. R. A. Haugerud and M. J. Kunk, *U.S. Geol. Surv., Open-File Rep. 88-261* (1988).
23. I. McDougall and T. M. Harrison, *Geochronology and Thermochronology by the $^{40}Ar/^{39}Ar$ Method* (Oxford Univ. Press, New York, 1988).
24. Our samples were separated from the bulk rock with standard heavy liquid and magnetic separation techniques. The purity of our separated grains determined in oil immersion mounts is estimated to be >99% except as noted. The grains that we analyzed were 150 to 180 μm in size.
25. D. Stewart, written communication.
26. E. K. Jessberger and R. Ostertag, *Geochim. Cosmochim. Acta* **46**, 1465, 1471 (1982).
27. T. M. Harrison and I. McDougall, *ibid.*, p. 1811.
28. The temperature range over which the samples released the bulk of their gas is lower than is common for most maximum microcline. The most likely cause for this is a nonhomogeneous effective reduction in grain radius for diffusion attributed to hypervelocity shock.
29. G. Turner, in *Origin and Distribution of the Elements*, L. H. Ahrens, Ed. (Pergamon, Oxford, 1968).
30. R. A. Haugerud and M. J. Kunk, in preparation.
31. A. R. Gillespie, J. C. Huneke, G. J. Wassenburg, *J. Geophys. Res.* **87**, 9247 (1982).
32. W. B. Harland *et al.*, *A Geologic Time Scale* (Cambridge Univ. Press, Cambridge, 1982); A. Hallam, J. M. Hancock, J. L. Labrecque, W. Lowrie, J. E. T. Channell, in *The Chronology of the Geological Record*, N. J. Snelling, Ed. (Memoir 10, Blackwell, New York, 1985); G. S. Odin, D. Curry, N. H. Gale, W. J. Kennedy, in *Numerical Dating in Stratigraphy*, G. S. Odin, Ed. (Wiley, New York, 1982).
33. J. D. Obradovich, J. F. Sutter, M. J. Kunk, *Terra Cognita* **6**, 140 (1986).
34. E. C. Alexander *et al.*, *U.S. Geol. Surv. Open-File Rep. 78-701* (1978), p. 6.
35. The isotopic composition of argon was measured with VG-Isotopes MM 1200B mass spectrometer at the U.S. Geological Survey in Reston, VA. The detection limit of the mass spectrometer at the time of these analyses was $4 \times 10^{-16}$ moles. Samples were irradiated in the Central Thimble facility of the U.S. Geological Survey TRIGA reactor in Denver, CO, and the $(^{36}Ar/^{39}Ar)Ca$, $(^{39}Ar/^{37}Ar)Ca$, and $(^{40}Ar/^{39}Ar)K$ ratios used were those reported by Dalrymple *et al.* (*21*). The monitor mineral used in this study was MMHb-1 which has an accepted age of 519.4 ± 0.5% (*34*). All $^{40}Ar$-$^{39}Ar$ ages were calculated with program Ar Ar* (*22*) and with the decay constants recommended by R. H. Steiger and E. Jaeger [*Earth Planet. Sci. Lett.* **36**, 359 (1977)].
36. We thank R. Anderson for supplying the samples, B. Dalrymple, E. Shoemaker, and D. Milton for constructive comments on the manuscript, B. Jackson for word processing, and A. Heine for his invaluable assistance in the lab. Authorized by the Director of the U.S. Geological Survey.

6 February 1989; accepted 15 May 1989